online data

Protein tyrosine phosphatase hPTPN20a is targeted to sites of actin polymerization

Michelle T. FODERO-TAVOLETTI*[1], Matthew P. HARDY*[2], Brent CORNELL*, Frosa KATSIS†, Christine M. SADEK*, Christina A. MITCHELL*, Bruce E. KEMP†‡ and Tony TIGANIS*[3]

*Department of Biochemistry and Molecular Biology, Monash University, Melbourne, Victoria 3800, Australia, †St. Vincent's Institute of Medical Research, Melbourne, Victoria 3065, Australia, and ‡CSIRO Health Sciences and Nutrition, Parkville, Victoria 3052, Australia

The human genome encodes 38 classical tyrosine-specific PTPs (protein tyrosine phosphatases). Many PTPs have been shown to regulate fundamental cellular processes and several are mutated in human diseases. We report that the product of the *PTPN20* gene at the chromosome locus 10q11.2 is alternatively spliced to generate 16 possible variants of the classical human non-transmembrane PTP 20 (hPTPN20). One of these variants, hPTPN20a, was expressed in a wide range of both normal and transformed cell lines. The catalytic domain of hPTPN20 exhibited catalytic activity towards tyrosyl phosphorylated substrates, confirming that it is a *bona fide* PTP. In serum-starved COS1 cells, hPTPN20a was targeted to the nucleus and the microtubule network, co-localizing with the microtubule-organizing centre and intracellular membrane compartments, including the endoplasmic reticulum and the Golgi apparatus. Stimulation of cells with epidermal growth factor, osmotic shock, pervanadate, or integrin ligation targeted hPTPN20a to actin-rich structures that included membrane ruffles. The present study identifies hPTPN20a as a novel and widely expressed phosphatase with a dynamic subcellular distribution that is targeted to sites of actin polymerization.

Key words: actin, alternative splicing, membrane ruffle, microtubule, protein tyrosine phosphatase (PTP).

INTRODUCTION

Protein tyrosine phosphorylation plays an integral role in many aspects of cellular signalling and controls diverse fundamental cellular responses, including growth, proliferation, differentiation, migration and survival [1]. Tyrosine phosphorylation is a reversible and dynamic process that is controlled by the activities of the PTKs (protein tyrosine kinases), which mediate the phosphorylation reaction, and the PTPs (protein tyrosine phosphatases), which catalyse the dephosphorylation [1]. The human genome encodes approx. 100 PTP genes [1–3], including 38 classical tyrosine-specific PTPs that contain catalytic domains of ~280 residues with the signature motif (I/V)HCSXGXGR(S/T)G [2,3]. The 38 classical PTPs can be subdivided further into 21 receptor-like transmembrane PTPs and 17 intracellular non-transmembrane PTPs. The catalytic domains of the classical PTPs share an overall sequence identity of approx. 35 %, whereas the non-catalytic regions are distinct and serve targeting/regulatory roles and, in the case of receptor-like PTPs, may bind ligand [1,2]. Many PTP gene products are alternatively spliced to generate variant proteins, often with distinct non-catalytic regions dictating subcellular localization, substrate recognition and regulation [1–3]. As such, the number of functionally distinct PTPs greatly exceeds the number identified in the human genome.

While PTKs have been studied intensively over the last few decades, less emphasis has been placed on characterizing PTPs. PTPs are now known to display exquisite substrate selectivity/specificity *in vivo* and to regulate specific signal transduction events and physiological processes [1,3]. Importantly, PTPs can act not only to terminate cellular signalling, but also to initiate it. For example, PTPα can dephosphorylate the inhibitory CSK (C-terminal Src PTK) phosphorylation site in Src family PTKs [4,5], whereas SHP-2 (Src homology region 2-containing PTP-2) controls CSK access to Src [6]. In accordance with the central role of PTPs in modulating physiological responses, mutation of PTPs or perturbation of PTP function can contribute to the development of varied human diseases, including cancer [7–10], diabetes [11–13], immune disorders [14] and heart disease [15]. Moreover, PTP mutations can be causative in disease onset, and, for example, heterozygous mice harbouring a Noonan-associated SHP-2 mutation exhibit the major features of the disease, including short stature, craniofacial abnormalities and heart defects [15], whereas somatic SHP-2 mutations that are common in sporadic leukaemias are transforming and can cause lymphoproliferation [9,10]. In

Abbreviations used: AMV, avian myeloblastosis virus; COP, coatamer protein; CSK, C-terminal Src protein tyrosine kinase; DMEM, Dulbecco's modified Eagle's medium; EGF, epidermal growth factor; EGFR, EGF receptor; ERC, endocytic recycling compartment; EST, expressed sequence tag; FBS, foetal bovine serum; GFP, green fluorescent protein; GFR, growth-factor-reduced; GST, glutathione S-transferase; HA, haemagglutinin; HEK, human embryonic kidney; *HSA*, *Homo sapiens*; HUVEC, human umbilical vein endothelial cell; MTOC, microtubule-organizing centre; ORF, open reading frame; PDI, protein disulphide-isomerase; poly(A)$^+$, polyadenylated; PTK, protein tyrosine kinase; PTP, protein tyrosine phosphatase; (h)PTPN20, (human) non-transmembrane PTP 20; RACE, rapid amplification of cDNA ends; RCML, reduced carboxyamidomethylated and maleylated lysozyme; RPTP, receptor-type PTP; RT, reverse transcriptase; SHP-2, Src homology region 2-containing PTP-2; siRNA, small interfering RNA; STEP, striatal enriched phosphatase; STYX, phosphoserine/threonine/tyrosine-interacting; TCPTP, T-cell PTP; TC45, 45 kDa variant of TCPTP; TdT, terminal deoxynucleotidyl transferase; UTR, untranslated region; VSVG, vesicular stomatitis virus glycoprotein.

[1] Present address: Department of Pathology, The University of Melbourne, Parkville, Victoria 3052, Australia.

[2] Present address: CSL Ltd, Parkville, Victoria 3052, Australia.

[3] To whom correspondence should be addressed (email Tony.Tiganis@med.monash.edu.au).

The nucleotide sequence data reported will appear in DDBJ, EMBL, GenBank® and GSDB Nucleotide Sequence Databases under the accession numbers AY704141, AY704142, AY704143, AY704144, AY704145, AY704146, AY704147, AY704148, AY704149, AY704150, AY704151, AY704152, AY704153, AY704154, AY704155, AY704156, AY704157, AY704158 and AY753191.

addition, pathogenic micro-organisms can target host PTPs for the modulation of tyrosine-phosphorylation-dependent signalling. Most notably, RPTPζ (receptor-type PTP) and SHP-2 are targeted by the *Helicobacter pylori* proteins VacA and CagA respectively, and mice lacking RPTPζ are resistant to ulceration induced by VacA [16,17]. Thus elucidating the functions of PTP family members is necessary to understand fully the regulation of signalling processes that involve reversible tyrosine phosphorylation and to provide comprehensive insight into the molecular mechanisms that underlie both physiological and pathological processes.

In the present paper, we report the cloning and characterization of hPTPN20, a classical human non-transmembrane PTP. Alternative splicing of the *PTPN20* gene product can result in the expression of at least 22 mRNA transcripts encoding 16 possible hPTPN20 variants. One of the novel variants, hPTPN20a, is widely expressed and has a dynamic subcellular distribution being targeted to sites of actin polymerization in response to varied extracellular stimuli.

MATERIALS AND METHODS

Materials

Recombinant human EGF (epidermal growth factor), GFR (growth-factor-reduced) Matrigel® matrix and dispase were purchased from Becton Dickinson (Bedford, MA, U.S.A.). Rabbit anti-EGF receptor (sc-03) and goat anti-actin (sc-1616) antibodies were from Santa Cruz Biotechnology (Santa Cruz, CA, U.S.A.); mouse anti-α-tubulin, anti-β-COP (coatamer protein) and anti-clathrin antibodies from Sigma (St. Louis, MO, U.S.A.) and mouse anti-nucleoporin p62 antibody from BD Transduction Laboratories (San Jose, CA, U.S.A.). The following reagents were supplied by colleagues: monoclonal anti-TCPTP (TCPTP is T-cell PTP) antibody CF4 by Dr N. K. Tonks (Cold Spring Harbor Laboratory, Cold Spring Harbor, NY, U.S.A.), monoclonal anti-HA (haemagglutinin) antibody 12CA5 by Dr J. Heierhorst (St. Vincent's Institute of Medical Research), ts045-VSVG–GFP [where ts045 is a mutant strain of VSVG (vesicular stomatitis virus glycoprotein) and GFP is green fluorescent protein] construct by Dr J. Lippincott-Schwartz (Cell Biology and Metabolism Branch, National Institutes of Health, Bethesda, MD, U.S.A.), pEGFP-Rab11 and pEGFP-Rab6 by Dr T. Rowe (Department of Biochemistry and Molecular Biology, Monash University). Total human testis RNA was a gift from Dr K. Loveland (Monash Institute of Reproduction and Development, Monash University).

Differential display

Total RNA was isolated from asynchronous ECV304 cells, or those differentiated on GFR Matrigel® matrix, using the RNeasy RNA extraction kit (Qiagen GmbH, Hilden, Germany) according to the manufacturer's recommendations; differentiated ECV304 cells were isolated by solubilizing the GFR Matrigel® matrix with dispase (37 °C for 30 min). Total RNA was then reverse-transcribed using AMV (avian myeloblastosis virus) RT (reverse transcriptase) (Roche Diagnostics GmbH, Mannheim, Germany), 5 μg of total RNA and 0.5 μg of oligo(dT)$_{15}$ (Roche Diagnostics) in a final volume of 25 μl, according to the manufacturer's instructions. One-tenth of this reaction mixture was then used for amplification of PTP cDNAs using 25 pmol of each of the forward [NPTP-1 5′-CTCTGGATCCACIGA(C/T)TA(C/T)AT(A/C/T)-AA(C/T)GC-3′, where I is inosine] and reverse [NPTP-2; 5′-CTC-TAAGCTTC(G/T)ICCIA(T/C)ICCI(C/G)(T/A)(A/G)CA(G/A)-TG-3′] degenerate oligonucleotide primers with 4 μCi of [α-^{35}S] dATP (Amersham Biosciences, Little Chalfont, Buckinghamshire, U.K.) and Taq DNA polymerase (Roche Diagnostics) in a final volume of 20 μl, according to the manufacturer's recommendations. Cycling conditions were as follows: 94 °C for 5 min, followed by 40 cycles of 94 °C for 30 s, 40 °C for 60 s and 72 °C for 30 s, followed by a final 10 min extension at 72 °C. PCR products were purified, digested with Sau96I, then separated on a 6 % bisacrylamide gel and analysed by autoradiography. DNA fragments of interest were extracted from the gel, amplified further with the same primers and then cloned into pGEM®-T easy (Promega) and sequenced.

RACE (rapid amplification of cDNA ends)

cDNA was generated from human testis or ECV304 total RNA using the 5′ RACE System, version 2.0, from Invitrogen (Carlsbad, CA, U.S.A.). cDNA reverse-transcribed from 5 μg of RNA was first treated with 0.5 μg/μl RNase (DNase-free) (Invitrogen) for 1 h at 37 °C, then incubated at 37 °C for a further 20 min in the following reaction to tail cDNAs: 5 μl of cDNA, 1 μl of 15 units/μl TdT (terminal deoxynucleotidyl transferase), 5 μl of 5× TdT buffer (Promega), 2.5 μl of 2.5 mM dCTP and 11.5 μl of water. The reaction was then inactivated at 70 °C for 10 min. The primary 5′ RACE reaction consisted of 2.5 μl of the dC-tailed cDNA, 1 μl of 5 mM dNTPs, 1.5 μl of 25 mM $MgCl_2$, 2.5 μl of 10× Taq buffer, 0.25 μl of 5 units/μl Taq DNA polymerase (Promega), 0.8 μl of 10 μM *PTPN20* gene-specific primer NPTP-3 (5′-CCAGAGTAGAACTCACCAGGC-3′; encoded by exon 7) and AAP (abridged anchor primer; 5′-GGCCACGC-GTCGACTAGTACGGGIIGGGIIGGGIIG-3′, where I is inosine), and the mixture was made to 25 μl with water. RACE PCR cycling conditions were 94 °C for 5 min, followed by 10 cycles of 92 °C for 1 min, 60 °C for 1 min and 72 °C for 2 min, and then 20 cycles of 92 °C for 1 min, 50 °C for 1 min and 72 °C for 2 min, with a final 10 min extension at 72 °C. Nested 5′ RACE reactions using 2.5 μl of a 1:10 dilution of the primary PCR product in a final volume of 25 μl were then performed with the 'nested' gene-specific primer NPTP-4 (5′-CTTGATGGCTGTCTGCTCA-3′; encoded by exon 6) and an AUAP (abridged universal amplification primer; 5′-GGCCACGCGTCGACTAGTAC-3′) and the following PCR cycling conditions: 94 °C for 5 min, followed by 30 cycles of 92 °C for 1 min, 50 °C for 1 min and 72 °C for 2 min, and a final 10 min extension at 72 °C. PCR products were cloned into pGEM®-T easy and sequenced.

RT-PCR analysis of PTPN20 isoform expression

Total RNA was extracted from 5×10^6 cells of the indicated cell line using TRI Reagent® (Sigma), according to the manufacturer's recommendations. cDNA was then generated from cells or human testis total RNA using Superscript™ III reverse transcriptase (Invitrogen) according to the manufacturer's recommendations. PCR from reverse-transcribed cDNA was performed using Taq DNA polymerase. Forward primers used for *PTPN20* RT-PCR reactions were NPTP-5 (5′-CTGTGGCTCTGTGGTAGGGGAAT-3′; encoded by exon 1b), NPTP-7 (5′-TGGCCTGACTCACAGGACA-CTAAG-3′; encoded by exon 2), NPTP-8 (5′-ATGATTGTAAA-CGATTATGAG-3′; encoded by exon 1b/3), NPTP-9 (5′-GCC-TGGTGAGTTCAACTCTGG-3′; encoded by exon 7) and NPTP-10 (5′-CCAGCTGCACTGTGACGCGTGTTG-3′; encoded by exon 1b). Reverse primers used were NPTP-3, NPTP-6 (5′-GT-GCAAACCCACTTGGTAATTTCA-3′; encoded by exon 11) and NPTP-11 (5′-CTCCTCATCCTCACTGCTCC-3′; encoded by exon 5). PCR cycling conditions were 94 °C for 2 min, followed by 45 cycles of 94 °C for 30 s; 60 °C for 30 s; 72 °C for 2 min, then a final 72 °C extension for 5 min. Amplified products were subcloned into pGEM-T easy (Promega) and sequenced. For the

β-actin RT-PCR, forward and reverse primers were 5′-TGAAGTCTGACGTGGACATC-3′ and 5′-ACTCGTCATACTCCTGCTTG-3′ respectively.

Sequence analysis

The complete nucleotide sequence of the human *PTPN20* gene and flanking regions was obtained from approx. 700 kb of human genomic DNA contained within a contig (NT_030772) encompassing part of *Homo sapiens* (*HSA*) chromosome locus 10q11.22. This sequence was obtained from the NCBI (National Center for Biotechnology Information) human genomic database found at http://www.ncbi.nlm.nih.gov, following BLAST analysis with identified cDNAs. Other sequences used in this study were also obtained from GenBank®: human *PTPN20* cDNAs BC036539, AL050040 and BX648913 which were derived from cDNA clones DKFZp566K0524 and DKFZp686N22268; human EST (expressed sequence tag) sequence BI460524 and the putative human *PTPN20* pseudogene XM_374802 (LOC399762). Identification of transcribed nucleotide sequences was performed using the NIX application (http://www.hgmp.mrc.ac.uk). Translation of putative ORFs (open reading frames) was carried out on the Baylor College of Medicine website (http://searchlauncher.bcm.tmc.edu), and amino acid alignments were performed using ClustalW 1.8 (http://www.ebi.ac.uk/clustalw/). Predictions of protein domains, as well as putative PEST (Pro-Glu-Ser-Thr) sequences and phosphorylation sites, were determined using PROSITE (http://www.expasy.ch/prosite/).

Northern blotting

Northern blots were carried out using a multiple tissue human poly(A)$^+$ (polyadenylated) RNA Northern blot [2 μg of poly(A)$^+$ RNA per lane; OriGene Technologies, Rockville, MD, U.S.A.] and ULTRAhyb™ hybridization buffer (Ambion, Austin, TX, U.S.A.), according to the manufacturer's recommendations (OriGene Technologies). Blots were pre-hybridized for 2.5 h and then hybridized at 42 °C for 20 h with a 750 bp [α-^{32}P]dCTP-labelled ($\sim 2 \times 10^8$ c.p.m./μg of cDNA) *PTPN20* cDNA fragment (nt 449–1198 of cDNA AL050040) corresponding to exons 7–11 of the *PTPN20* gene (see Supplementary Figures 2 and 3 at http://www.BiochemJ.org/bj/389/bj3890343add.htm). Blots were then washed with 2× SSC (1× SSC is 0.15 M NaCl/0.015 M sodium citrate)/0.1 % SDS twice at 42 °C for 15 min each and then 0.25× SSC/0.1 % SDS twice at 65 °C twice for 15 min each, and then exposed on a PhosphorImager using ImageQuant software (Molecular Dynamics). Blots were re-hybridized with the β-actin probe provided by the manufacturer (OriGene Technologies).

Plasmid constructs

The TC45-pMT2 (where TC45 is the 45 kDa variant of TCPTP) mammalian expression construct has been described previously [18]. hPTPN20a-pDrive was generated in a two-step PCR procedure using Platinum® Pfx DNA polymerase (Invitrogen, Carlsbad, CA, U.S.A.) and cDNA template that had been reverse-transcribed using AMV-RT and human testes RNA as described above. In the first round of PCR, two overlapping PCR fragments encompassing the 5′ and 3′ ends of hPTPN20a were amplified. The 5′ end was generated using 5′-CGCCGCGAATTCATGATTGTAAACGATTATGAG-3′ and 5′-TGAAGCTATCTGC TGAGGCA-3′, and the 3′ end was generated with 5′-TGCCTCAGCAGATAGCTTCA-3′ and 5′-CAGAAGTCTAGATTAATCCAAAGTCAGAAGTTTCCG-3′. For the second round of PCR, the corresponding 5′ and 3′ primers and a 1:1 molar ratio of the primary PCR products were utilized to generate the full-length hPTPN20a cDNA, which was then cloned into pDrive (Qiagen) as per the manufacturer's instructions. hPTPN20a cDNA was then PCR-amplified with Platinum® Pfx DNA polymerase using hPTPN20a-pDrive as a template. The 5′ primer (5′-CGCCGCGAATTCATGATTGTAAACGATTATGAG-3′) incorporated an EcoRI site immediately before the ATG initiation codon, and the 3′ primer (5′-CCGGCGGAATTCTCATCCTCCCAGGCTGGCATAGTCAGGACGTCATAAGGATAGCTATCCAAAGTCAGAAGTTTCCG-3′) incorporated a sequence for an in-frame HA tag before a TGA stop codon that was followed by a an EcoRI site. The EcoRI-digested PCR product was cloned into the same site of pMT2 to generate hPTPN20a-HA-pMT2, with the orientation being confirmed by restriction endonuclease digestion. A similar approach was used for cloning ΔN-term-pMT2, but the 5′ primer (5′-CGCCGCGAATTCATGGGCCCCTTCAGAAGAGACAGGTGGA-3′) incorporated an EcoR1 site followed by ATG immediately before the codon for residue 78 of hPTPN20a instead. The hPTPN20a-HA-pCG construct was generated by PCR using Platinum® Pfx DNA polymerase and the hPTPN20a-HA-pMT2 construct as template. The 5′ primer (5′-CGCCGCTCTAGAATGATTGTAAACGATTATGAG-3′) incorporated an SpeI site immediately 5′ to the initiating codon, and the 3′ primer was the same as that used above that incorporated sequence for a HA tag, but instead included a BamH1 site rather than an EcoRI site. The SpeI/BamH-digested PCR product was cloned into the XbaI/BamHI site of the mammalian expression vector pCG. hPTPN20a (151–411)-pGEM®-T easy was generated by RT-PCR using AMV-RT, Taq DNA polymerase and human testes RNA. The 5′ oligonucleotide primer (5′-GAGGAGGGATCCATGCAGGAATTTATGGCTTTAGAAC-3′) incorporated a BamHI site immediately before the ATG initiation codon and the 3′ oligonucleotide (5′-CAGAAGTCTAGATTAATCCAAAGTCAGAAGTTTCCG-3′) incorporated an XbaI site immediately following the TAA stop codon. The resulting PCR product was cloned into pGEM®-T easy according to the manufacturer's instructions. hPTPN20a (151–411)-pGEX for the bacterial expression of GST (glutathione S-transferase)–hPTPN20a (151–411) was generated by subcloning the BamHI/XbaI-digested insert from hPTPN20a (151–411)-pGEM®-T easy into the same sites of pGEX-KG. For generating the construct expressing the siRNA (small interfering RNA) corresponding to sequence in exon 6 (see Supplementary Figures 2 and 3 at http://www.BiochemJ.org/bj/389/bj3890343add.htm) and capable of suppressing endogenous hPTPN20 expression in mammalian cells, the oligonucleotides 5′-GATCCCCCTAGATCAGTTGGCTCAGATTCAAGAGATCTGAGCCAACTGATCTAGTTTTTGGAAA-3′ and 5′-AGCTTTTCCAAAAACTAGATCAGTTGGCTCAGATCTCTTGAATCTGAGCCAACTGATCTAGGGG-3′ were annealed, phosphorylated with T4 polynucleotide kinase and cloned into a BglII/HindIII site of pSUPER as described previously [19]. The structures of all the constructs generated were confirmed by restriction endonuclease analysis and the fidelity of the cloned cDNAs confirmed by sequencing.

Antibodies

Rabbit polyclonal 159 antibodies against TC45 were described previously [20]. Rabbit polyclonal anti-hPTPN20 antibodies were raised against the peptide C^{162}LPGEFYSGNQPSNREK^{177}-NH_2 (TT2) corresponding to the N-terminus of the hPTPN20a catalytic domain and Y^{393}HFCYDIVLEVLRKLLTLD^{411}-COOH (TT3) corresponding to the hPTPN20a C-terminus. Rabbits were immunized with the peptides coupled to keyhole-limpet haemocyanin using SPDP ([*N*-succinimidyl 3-(2-pyridyldithio)propionate] (Pierce, Rockford, IL, U.S.A.). Antibodies specific for the immunized peptides TT2 and TT3 were purified from serum

using the corresponding peptide affinity columns and were avidity-characterized by ELISAs, immunoblot analysis and immunofluorescence microscopy. TT2 antibodies recognized overexpressed hPTPN20a–HA, whereas TT3 antibodies recognized endogenous hPTPN20a by immunoblot analysis.

Cell culture and transfections

African-green-monkey COS1 and HEK (human embryonic kidney)-293 cells, as well as human HeLa cervical adenocarcinoma, U2OS osteosarcoma, U87MG glioblastoma, MDA-MB-231 breast adenocarcinoma and ECV304 urinary carcinoma [21,22] cells were cultured at 37 °C and 5 % CO_2 in DMEM (Dulbecco's modified Eagle's medium) (Invitrogen) containing 5 % (v/v) FBS (foetal bovine serum), 100 units/ml penicillin and 100 μg/ml streptomycin. Human MRC5 and 7625 normal fibroblasts were cultured in the same medium containing 10 % (v/v) FBS plus antibiotics, whereas Jurkat T-cells were cultured in RPMI 1640 medium (Invitrogen) containing 10 % (v/v) FBS plus antibiotics. All cell lines were from the A.T.C.C. (American Type Culture Collection; Manassas, VA, U.S.A.). Where indicated, cells were serum-starved in medium containing 0.1 % (v/v) FBS plus antibiotics for 20 h.

COS1 or HeLa cells were electroporated with pMT2 or hPTPN20a-HA-pMT2 as described previously [23,24]. Cells were collected for immunofluorescence microscopy or in hot 3× Laemmli sample buffer for immunoblotting at 36 h post-transfection as indicated. Where indicated, hPTPN20a–HA expressing serum-starved COS1 cells were harvested by limited trypsin/EDTA treatment, washed twice in DMEM minus Phenol Red (Invitrogen) containing 0.25 % (w/v) BSA, and then resuspended in DMEM minus Phenol Red containing 0.1 % (w/v) BSA. The cells were held in suspension at 37 °C for 30 min before attachment on to coverslips pre-coated with 20 μg/ml fibronectin (Sigma) for 10–30 min as described previously [23].

Cell fractionation studies

Where indicated, COS1 cells were electroporated with pMT2 or hPTPN20a-HA-pMT2 and used at 36 h post-transfection. Subcellular fractionation was performed according to the method of Simpson et al. [25]. In brief, cells were washed with ice-cold PBS, homogenized using a mechanical homogenizer in pre-chilled HES buffer (20 mM Hepes, pH 7.2, 0.225 M sucrose and 1 mM EDTA) plus protease inhibitors [pepstatin (1 μg/ml), leupeptin (5 μg/ml), aprotinin (5 μg/ml), 1 mM benzamidine and 2 mM PMSF], and the homogenate was centrifuged (11 500 rev./min at 4 °C for 25 min, using a Sorval SS34 rotor). The supernatant then underwent two additional rounds of centrifugation (15 500 rev./min at 4 °C for 45 min using a Sorval SS34 rotor, followed by 55 000 rev./min at 4 °C for 1 h using a Beckman Ti70 rotor). The first centrifugation step produced the high-density microsome fraction (pellet); the second centrifugation step produced the cytosolic fraction (supernatant) and the low-density microsome fraction (pellet). The pellet resulting from the original centrifuged homogenate, containing nuclei, mitochondria, endoplasmic reticulum and plasma membrane, was resuspended in HES buffer and homogenized further using a Dounce homogenizer. The homogenate was then layered on to a sucrose cushion and centrifuged (28 500 rev./min at 4 °C for 1 h using a Beckman SW41 rotor); the resulting pellet containing nuclei, as well as mitochondria and endoplasmic reticulum, was retained for analysis, whereas the interphase fraction was resuspended in HES buffer and re-centrifuged (50 000 rev./min at 4 °C for 15 min using a Beckman Ti60 rotor) to pellet the plasma membrane/endoplasmic reticulum fraction. Equal amounts of protein were resolved by SDS/PAGE (12 % polyacrylamide) and analysed by immunoblot analysis.

Microtubule binding assay

HeLa cells were electroporated with 5 μg of pCG or hPTPN20a-HA-pCG and at 36 h post-transfection, were left untreated, treated with 5 μM taxol at 37 °C for 4 h or treated with 10 μM nocodazole at 37 °C for 2 h followed by incubation at 4 °C for 2 h. Cells were washed with PBS and incubated in microtubule stabilizing buffer [0.1 M Pipes, pH 6.9, 2 M glycerol, 5 mM $MgCl_2$, 2 mM EGTA and protease inhibitor cocktail (Roche Diagnostics)] for 5 min at 37 °C to extract proteins. Cells were collected, an aliquot was removed (total fraction), and the remainder was centrifuged at 1000 ***g*** for 2 min. The supernatant was removed (cytosolic proteins), and the pellet (microtubule fraction) was treated with DNase I for 5 min at 37 °C. Proteins were resolved by SDS/PAGE (10 % polyacrylamide) and immunoblotted with antibodies against tubulin or HA (12CA5).

Immunofluorescence microscopy

For immunofluorescence studies, cells overexpressing hPTPN20–HA grown on glass coverslips were fixed with 3.2 % (w/v) paraformaldehyde in PBS and were processed as described previously [18] using the monoclonal anti-HA antibody 12CA5 or the polyclonal anti-hPTPN20 TT2 antibodies on their own, or in combination with antibodies against β-COP, clathrin or tubulin. Where indicated, cells were co-transfected with constructs for the expression of GFP–Rab11 or VSVG–GFP. Alexa Fluor® 488- or 568-conjugated goat anti-mouse or anti-rabbit IgGs (Molecular Probes, Eugene, OR, U.S.A.) were used as secondary antibodies. Where indicated, cells were stained with Texas-Red Phalloidin (Molecular Probes) to visualize the actin cytoskeleton. For staining DNA, cells were incubated with 5 μg/ml RNase (Roche Diagnostics) in PBS for 30 min and then incubated with propidium iodide in PBS containing RNase for 15 min and then washed with PBS. Where indicated, nuclei were visualized with Hoechst stain. Coverslips were mounted on to glass slides in Dako® fluorescent mounting medium (Dako Corporation, Carpinteria, CA, U.S.A.), and immunofluorescence was visualized on a Zeiss Axioskop 2 mot plus microscope or a Leica TCS-NT confocal microscope.

Metabolic labelling and pulse–chase

COS1 cells were electroporated as described previously [23] with 10 μg of hPTPN20a-HA-pMT2 or ΔN-term-HA-pMT2 and were seeded in a six-well dish. At 20 h post-transfection, the cells were rinsed with PBS and starved in methionine-free DMEM plus 5 % FBS for 90 min. Cells were pulsed with 0.2 mCi of Trans ^{35}S-label per well for 2 h and chased in DMEM plus 10 % FBS for 0–24 h. Cells were lysed in immunoprecipitation lysis buffer [50 mM Tris/HCl, pH 7.5, 1 % (w/v) Nonidet P40, 150 mM NaCl, 50 mM NaF, leupeptin (5 μg/ml), pepstatin (1 μg/ml), 1 mM benzamidine and 2 mM PMSF) and pre-cleared with 0.1 ml Pansorbin for 30 min at 4 °C. Pre-cleared lysates were centrifuged (12 000 ***g*** for 10 min at 4 °C) and hPTPN20a–HA or ΔN-term-HA was immunoprecipitated from the supernatant with the monoclonal anti-HA 12CA5 antibody as described previously [18]. 12CA5 immunoprecipitates were resolved by SDS/PAGE (10 % polyacrylamide) and [^{35}S]methionine-labelled hPTPN20a-HA or ΔN-term-HA quantified on a PhosphoImager using ImageQuant software.

PTP assays

GST and GST–hPTPN20a (151–411) proteins were expressed in bacteria and purified on glutathione–Sepharose as described

previously [20,26]. RCML (reduced carboxyamidomethylated and maleylated lysozyme) was phosphorylated with the baculoviral expressed PTK domain of the human insulin receptor [27]. PTP activity was measured as described previously [20,26] using 20 μM tyrosine-phosphorylated ^{32}P-labelled RCML at 30 °C for 10–20 min in reaction buffer containing 25 mM imidazole, pH 7.2, 5 mM EDTA, 1 mM dithiothreitol and 1 mg/ml BSA. No more than 20 % of the substrate was dephosphorylated in each reaction.

RESULTS

Identification of a human PTPN20 cDNA fragment

In an attempt to identify novel PTPs that may be involved in the formation of endothelial tube-like structures we assessed PTP mRNA expression by differential display comparing asynchronous transformed ECV304 cells with the same cells differentiated into tube-like structures on Matrigel®. We used degenerate oligonucleotide primers corresponding to the amino acid sequences [S/T]DYINAS and HCSAG[I/V]GR that are conserved within classical PTP catalytic domains [2,3]. We identified several differentially expressed human cDNAs, including a cDNA encoding the transmembrane classical phosphatase PTPRJ (PTP receptor type J) [DEP-1 (density-enhanced phosphatase-1)] (M. T. Fodero-Tavoletti and T. Tiganis, unpublished work) which has been implicated previously in vascular development [28]. In addition, we identified other PTP cDNAs that were not differentially expressed, including a cDNA that was identical with a previously identified, but hitherto uncharacterized, human cDNA clone DKFZp566K0524 (GenBank® accession number AL050040) encoding non-transmembrane PTP 20 (PTPN20) and homologous with the catalytic domain of murine Typ expressed in testes (GenBank® accession number NM_008978) [29].

Alternative splicing of the human PTPN20 gene

We next performed a detailed examination of the human cDNA and EST databases using the identified human *PTPN20* catalytic domain cDNA sequence. Three cDNA/EST sequences were identified (GenBank® accession numbers BC036539, BI460524 and BX648913) encoding potential variants of human PTPN20 (hPTPN20) with deleted PTP domains; BI460524 and BX648913 encoded proteins with N-termini identical with AL050040, whereas BC036539 encoded a protein with an N-terminus similar to the murine Typ [29]. To identify full-length *PTPN20*, we performed 5′ RACE analysis of *PTPN20* using cDNA generated from ECV403 cell and human testis mRNA and primers (NPTP-3 and NPTP-4) corresponding to the AL050040 cDNA as described in the Materials and methods section. When sequenced, most RACE products (results not shown) identified a novel isoform of *PTPN20*, which differed from the others at its 5′ end and which we have designated *PTPN20a*.

In order to confirm the existence of the *PTPN20a* cDNA, RT-PCR was performed using human testis or ECV304 cDNA and primers specific for the *PTPN20a* 5′ end (NPTP-3 and NPTP-5). The *PTPN20a* RT-PCR reactions generated a 561 bp product which, when sequenced, confirmed the presence of this isoform (see Supplementary Figure 1A at http://www.BiochemJ.org/bj/389/bj3890343add.htm). To confirm that the *PTPN20a* cDNA encoded an intact PTP domain, the entire ORF of *PTPN20a* was amplified as a single 1284 bp product from ECV304 cDNA (see Supplementary Figure 1B at http://www.BiochemJ.org/bj/389/bj3890343add.htm), using the primers NPTP-5 and NPTP-6, and then sequenced to confirm identity. Although only a single PCR product was amplified from ECV304 cDNA, multiple PCR products were generated when full-length *PTPN20a* was amplified from testis cDNA (see Supplementary Figure 1C at http://www.BiochemJ.org/bj/389/bj3890343add.htm). These cDNAs were sequenced and were found to encode possible variants of hPTPN20a containing N-terminal alterations, or PTP catalytic domain deletions (see Supplementary Figure 2 at http://www.BiochemJ.org/bj/389/bj3890343add.htm).

Other products generated by 5′ RACE corresponded to *PTPN20* cDNA sequence AL050040, or the BC036539 sequence that did not encode an intact PTP catalytic domain. As indicated above, BC036539 encodes a predicted protein with similarity to the N-terminus of Typ [29]. We therefore postulated that a human isoform with an intact catalytic domain and similarity to the Typ N-terminus might exist. To test this, RT-PCR was performed from a testis cDNA library using primers specific for the putative isoform aimed at amplifying an entire *PTPN20* ORF (NPTP-6 and NPTP-7). Two main PCR products of 837 bp and 1385 bp were generated (see Supplementary Figure 1D at http://www.BiochemJ.org/bj/389/bj3890343add.htm) which, when sequenced, corresponded to BC036539 and also a variant encoding an intact catalytic domain. We have designated the intact catalytic domain cDNA variant *PTPN20b* and the cDNA with the catalytic domain deleted (BC036539) *PTPN20b-1*. These sequences and others identified by RT-PCR are summarized in Supplementary Figure 2 (http://www.BiochemJ.org/bj/389/bj3890343add.htm) and have been deposited into GenBank® (see Supplementary Figure 2 for accession numbers).

Localization and annotation of the human PTPN20 gene

To identify and annotate the *PTPN20* gene, BLAST analysis of the human genomic DNA database was performed using the human *PTPN20* cDNA sequences. A region of identity was found on *HSA* chromosome locus 10q11.22. The human *PTPN20* gene encompasses approx. 92 kb of genomic DNA and is transcribed towards the centromere of *HSA* chromosome 10 (results not shown). A putative *PTPN20* pseudogene (LOC399762) encoding a protein of 120 amino acids with 92 % identity with the hPTPN20b N-terminus was identified approx. 500 kb downstream of *PTPN20* (results not shown). FISH (fluorescent *in situ* hybridization) analysis using a 778 bp cDNA probe corresponding to nucleotides 420–1197 of the human *PTPN20* cDNA (GenBank® accession number AL050040) confirmed the genomic localization of *PTPN20* to *HSA* chromosome locus 10q11.2 (results not shown). Annotation of the *PTPN20* gene shows that it is composed of 12 exons and 10 introns (see Supplementary Figure 3 at http://www.BiochemJ.org/bj/389/bj3890343add.htm). Exons 1a, 1b and 2 contain the 5′ UTRs (untranslated regions) of all isoforms. Exons 1a–6 encode the N-terminal portion of hPTPN20a; exons 6–11 encode the PTP domain, and exon 11 also encodes the entire 3′ UTR (see Supplementary Figure 3 at http://www.BiochemJ.org/bj/389/bj3890343add.htm). Intron sizes range from 244 bp (intron 1a) to $>$ 20 kb (intron 1b) (see Supplementary Figure 3 at http://www.BiochemJ.org/bj/389/bj3890343add.htm), and the intron–exon boundaries conform to the GT-AG rule [30] (results not shown). Several single nucleotide polymorphisms were also identified in the human *PTPN20* gene. Two occur in the 3′ UTR (T2030C and A2202C) of the *PTPN20a* cDNA and two within the coding region (T136C and A151G); however, only one polymorphism results in a predicted amino acid change (T21A). All the possible isoforms of hPTPN20 would be generated by alternative splicing with *PTPN20a*, *PTPN20b*, *PTPN20c* and *PTPN20d* (see Supplementary Figure 2 at http://www.BiochemJ.org/bj/389/bj3890343add.htm) encoding proteins with intact PTP catalytic domains.

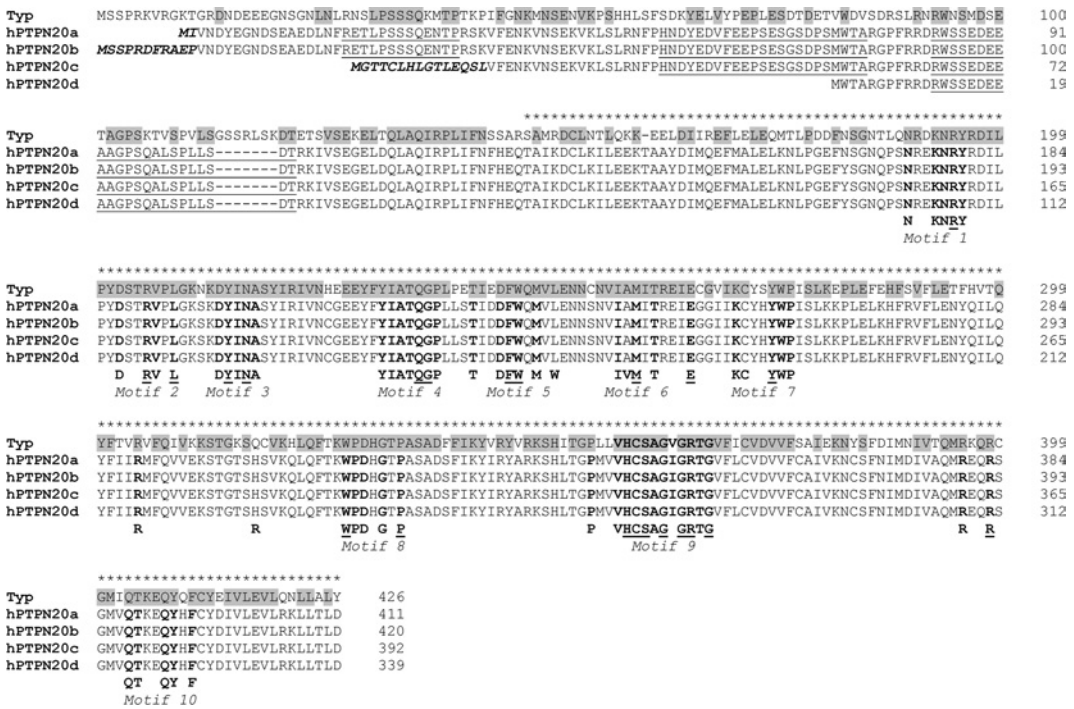

Figure 1 Amino acid alignment of hPTPN20 variants

ClustalW alignment of hPTPN20 variants a–d with the murine Typ sequence [29]. Regions of amino acid identity between hPTPN20 and Typ are highlighted on the Typ sequence in grey. Amino acids are numbered and the PTP catalytic domain [2] is indicated by asterisks above the sequence. Divergent hPTPN20 N-terminal amino acids are shown in bold italics and putative PEST sequences are underlined. Residues that are highly conserved in classical PTPs, including 22 invariant residues (underscored) that constitute the ten conserved PTP catalytic domain motifs [3], are indicated.

Characterization of the hPTPN20a protein

An alignment of the potential hPTPN20 full-length isoforms with the putative hPTPN20 murine homologue Typ is shown in Figure 1. Typ has an overall sequence identity of 66 % with its putative human orthologue hPTPN20b; the Typ and hPTPN20b catalytic domains are 74 % identical, whereas their non-catalytic N-termini are 52 % identical. This degree of identity is similar to that observed for closely related, but distinct, PTPs such as PTP1B and TCPTP (72 % identity, 86 % similarity; TCPTP catalytic domain residues 43–288), which have overlapping, but also unique, functions [1–3].

The catalytic domains of classical PTPs comprise ~280 residues and contain the signature motif (I/V)HCSXGXGR(S/T)G (motif 9; Figure 1) that includes the catalytically essential cysteine (Cys^{215} in PTP1B) and arginine residues, as well as nine other highly conserved motifs that include the WPD (Trp-Pro-Asp) loop (motif 8; Figure 1), which contains the invariant aspartate residue (Asp^{181} in PTP1B) that serves as a general acid–base catalyst, and the Q loop (motif 10; Figure 1) that contains the glutamine (Gln^{262} in PTP1B) that is involved in the second hydrolysis step of the phosphocysteine enzyme complex [1–3]. The signature motif sequence (VHCSAGIGRTG; amino acids 342–352 of hPTPN20a) and the other nine invariant PTP catalytic domain motifs are conserved in hPTPN20 (Figure 1). Consistent with this, a GST–hPTPN20a (151–411) fusion protein comprising the hPTPN20 catalytic domain dephosphorylated tyrosyl phosphorylated RCML *in vitro* (Figure 2A).

Although the predicted non-catalytic N-terminus of hPTPN20a does not exhibit any significant similarity to any known protein, three predicted PEST motifs were identified (residues 19–31, 54–76 and 87–104 in hPTPN20a) (Figure 1); PEST motifs can target proteins for proteolytic destruction [31]. The half-life of hPTPN20a as measured by [^{35}S]methionine pulse–chase labelling was approx. 1 h, which is short when compared with PTPs such as TCPTP, which has a half-life of 12–16 h [20]. Nonetheless, truncation of the first two predicted PEST motifs in hPTPN20a did not significantly alter protein half-life (Figure 2B), indicating that, on their own, the putative PEST motifs may not have a significant role in controlling hPTPN20a stability. The non-catalytic hPTPN20a N-terminus also contains numerous potential serine/threonine phosphorylation sites that may be important for regulation, but these were not examined in the present study.

Expression of human PTPN20

In order to identify tissues in which *PTPN20* may be expressed, Northern blot analysis was performed using a panel of human tissue mRNAs and a human *PTPN20* cDNA probe corresponding to the hPTPN20 catalytic domain (Figure 3A). Although not expressed abundantly, a single ~3.0 kb mRNA transcript was detected in human testis (Figure 3A) as reported previously for murine *Typ* [29]. However, since we identified *PTPN20* from human bladder cancer ECV304 epithelial cells, we reasoned that *PTPN20* might also be expressed in other human tissues and cell types, albeit at lower levels. Consistent with this, ESTs corresponding to *PTPN20* were identified from distinct sources, including pancreas (CA778311, BQ787020, CA778018, BG655503 and BQ786761), brain (BX648913 and CD108815) and aorta (D62174 and D79354).

We next compared the relative abundance of the *PTPN20* alternative spliced variants in different cell lines by RT-PCR analysis (Figure 3B). First, the expression of *PTPN20* cDNAs encoding proteins with intact PTP catalytic domains was assessed with specific oligonucleotide primers corresponding to exons 7 and 11

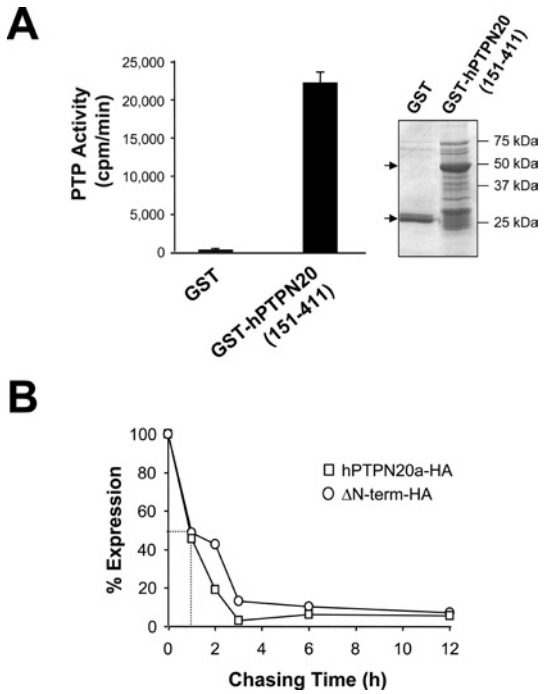

Figure 2 Characterization of hPTPN20 activity and protein stability

(**A**) The tyrosine phosphatase activities of GST–hPTPN20a (151–411) or GST control expressed in *Escherichia coli* and purified on glutathione–Sepharose were measured at 30 °C for 10 min with 10 μM ^{32}P-labelled RCML as substrate in 50 mM imidazole, pH 7.2, 0.1 % 2-mercaptoethanol and 1 mg/ml BSA. The experiment shown is representative of two independent experiments with triplicate transfections assayed in duplicate. Units shown are c.p.m. of ^{32}P released per min. The inset shows the purified GST or GST–PTPN20a (151–411) proteins resolved by SDS/PAGE (10 % polyacrylamide) and visualized by Coomassie Blue staining. (**B**) COS1 cells were electroporated with constructs for the expression of full-length hPTPN20a–HA, or ΔN-term–HA lacking the first two predicted PEST sequences and seeded into a six-well dish. At 20 h post-transfection, the cells were rinsed with PBS and starved in methionine-free DMEM plus 5 % FBS for 90 min. Cells were pulsed with 0.2 mCi of Trans ^{35}S-label per well for 2.5 h and chased in DMEM plus 10 % (v/v) FBS for 0–12 h. Cells were lysed in immunoprecipitation lysis buffer, pre-cleared with Pansorbin, and hPTPN20a–HA or ΔN-term–HA immunoprecipitated from the supernatant with antibodies against HA. Immunoprecipitates were resolved by SDS/PAGE (10 % polyacrylamide) and [^{35}S]methionine-labelled hPTPN20a–HA or ΔN-term–HA quantified on a PhosphoImager using ImageQuant software. Results are expressed as the percentage of the zero-time protein remaining at the time indicated on the *x*-axis. Shown is a representative experiment of two independent experiments.

(NPTP-9 and NPTP-6) (Figure 3B). An expected product of 751 bp was amplified from all the cell lines examined, including secondary cultures of HUVECs (human umbilical vein endothelial cells) (results not shown), normal MRC5 and 7625 fibroblasts, transformed HEK-293 epithelial cells and COS1 fibroblasts, and several tumour cell lines. Next we compared the expression of *PTPN20a* compared with that of *PTPN20b* or *PTPN20c*; *PTPN20a* was assessed with oligonucleotide primers specific to exons 1b/3 and 7 (NPTP-8 and NPTP-3) or exons 1b/3 to 11 (NPTP-8 and NPTP-6) and compared with the expression of *PTN20b* or *PTPN20c*, as assessed with primers specific to exons 2 and 11 (NPTP-7 and NPTP-6). *PTPN20a* was expressed in all human cell lines examined, whereas the expression of *PTPN20b* and *PTPN20c* and their corresponding truncation and deletion variants was more restricted and variable (Figure 3B). Notably, *PTPN20b* and *PTPN20c* were not present in some cell lines, including HUVECs (results not shown), ECV304 and HeLa cells (Figure 3B). For ECV304 cells, the absence of *PTPN20b* and *PTPN20c* isoforms was confirmed further using a different primer combination (NPTP-7 and NPTP-3; specific to exons 2 and 7

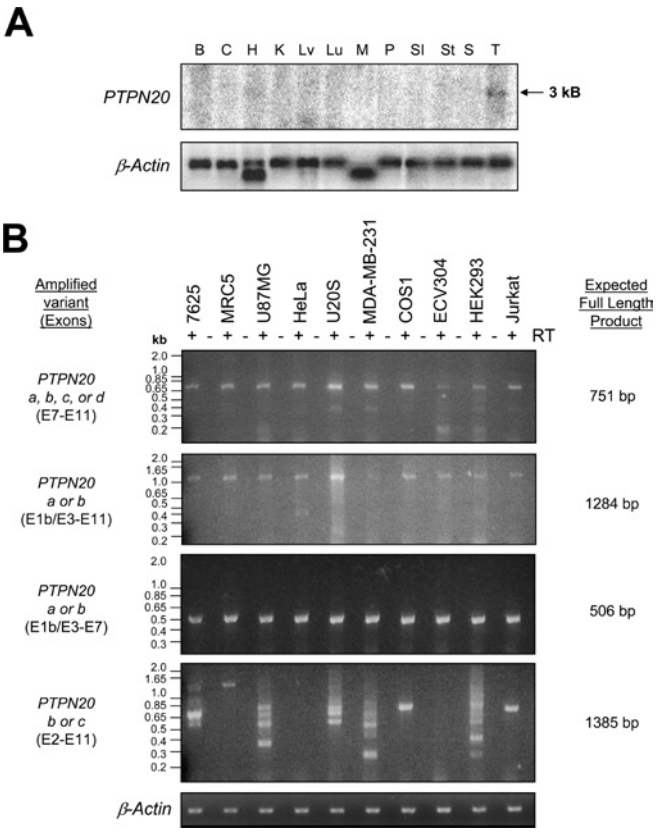

Figure 3 Northern blot and RT-PCR analysis of human PTPN20

(**A**) A multiple human tissue poly(A)$^+$ mRNA Northern blot hybridized with a ^{32}P-labelled *PTPN20* cDNA fragment encoding the PTP domain. The lower panel shows the same blot probed with ^{32}P-labelled β-actin cDNA. B, brain; C, colon; H, heart; K, kidney; Lv, liver; Lu, lung; M, skeletal muscle; P, placenta; SI, small intestine; St, stomach; S, spleen; T, testis. (**B**) RT-PCR of *PTPN20* cDNA from normal and transformed human cell lines. The top panel shows the amplification of a 751 bp cDNA encoding the hPTPN20 PTP catalytic domain using primers NPTP-9 and NPTP-6 (corresponding to exons 7 and 11 respectively; see Supplementary Figure 2 at http://www.BiochemJ.org/bj/389/bj3890343add.htm). The next panel shows the amplification of a 1284 bp cDNA encoding either hPTPN20a or hPTPN20b using primers NPTP-8 and NPTP-6 (corresponding to exons 1b/3 and 11 respectively; see Supplementary Figure 2 at http://www.BiochemJ.org/bj/389/bj3890343add.htm). The third panel shows the amplification of a 506 bp cDNA fragment encoding the N-termini of the hPTPN20a and hPTPN20b variants using primers NPTP-8 and NPTP-3 (corresponding to exons 1b/E3 and 7 respectively; see Supplementary Figure 2 at http://www.BiochemJ.org/bj/389/bj3890343add.htm). In the fourth panel, RT-PCR was performed using primers NPTP-7 and NPTP-6 (corresponding to exons 2 and 11 respectively; see Supplementary Figure 2 at http://www.BiochemJ.org/bj/389/bj3890343add.htm) to amplify an expected 1385 bp product encoding the full-length *PTPN20b* or *PTPN20c* variant. Minus-RT and β-actin controls are also shown.

respectively), which generated the expected 607 bp product from testis cDNA, but not from ECV304 cDNA (results not shown). These results indicate that *PTPN20a* might be expressed in varied cell types and, in some cell lines, *PTPN20a* represents the predominant form of the phosphatase.

To examine *PTPN20* expression further, polyclonal antibodies were generated against a peptide corresponding to the hPTPN20a C-terminus (TT3) that is present in all the predicted hPTPN-20 variant proteins with an intact catalytic domain (hPTPN20a, hPTPN20b, hPTPN20c and hPTPN20d), as well as in some of the catalytic domain deleted and/or truncated variants (hPTPN20a-1 and -2, hPTPN20b-2, hPTPN20d-1 and hPTPN20e) (see Supplementary Figure 2 at http://www.BiochemJ.org/bj/389/bj3890343add.htm). The expression of endogenous hPTPN20 was examined in a range of cell types by immunoblot analysis

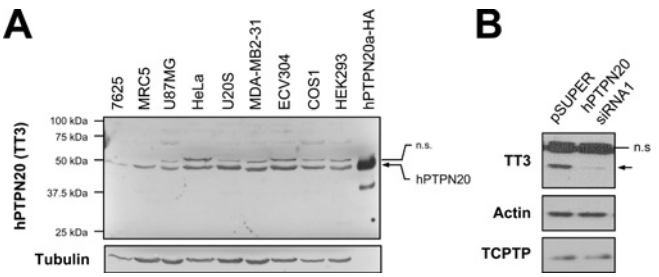

Figure 4 Expression analysis of hPTPN20 variants

(**A**) Lysates from the indicated cell lines as well as COS1 cells expressing hPTPN20a–HA were resolved by SDS/PAGE (10% polyacrylamide) and immunoblotted with anti-hPTPN20 TT3 polyclonal antibodies and then tubulin. Indicated is the electrophoretic mobility of hPTPN20 and that of a non-specific (n.s.) protein recognized by TT3. Molecular masses are given in kDa. (**B**) HEK-293 cells were electroporated with pSUPER vector control or pSUPER-siRNA1 expressing PTPN20 siRNA to suppress hPTPN20 expression. At 36 h post-transfection, cell lysates were resolved by SDS/PAGE (10% polyacrylamide) and immunoblotted with anti-hPTPN20 TT3 polyclonal antibodies and then antibodies against actin and TCPTP. Indicated is the electrophoretic mobility of hPTPN20 and that of a non-specific (n.s.) protein recognized by TT3.

(Figure 4A). A protein with an electrophoretic mobility that was consistent with the predicted molecular mass of either hPTPN20a (47.4 kDa) and identical with that of C-terminally HA-tagged hPTPN20a (hPTPN20a–HA) was expressed in different cell types, including both normal and immortalized/transformed cells (Figure 4A). This protein was not detected by the corresponding pre-immune serum antibodies (results not shown), and an siRNA corresponding to a sequence encoding the hPTPN20 non-catalytic N-terminus suppressed the expression of this protein without altering the expression of actin, the tyrosine phosphatase TCPTP or another non-specific immunoreactive 50 kDa protein (Figure 4B) that was variably recognized by the TT3 antibody. Significant levels of other predicted hPTPN20 variants including the catalytic domain deleted and/or truncated variants were not detected in the cell lines tested. Therefore, taken together with the RT-PCR analyses in Figure 3(B), these results indicate that the hPTPN20a protein may predominate in cells *in vitro*.

Subcellular localization of hPTPN20a

Having established that the hPTPN20a variant may predominate in varied cell types, we next sought to assess its subcellular distribution. The recognition of a non-specific protein by the TT3 antibody by Western blot analysis (Figure 4) prohibited its use for assessment of endogenous hPTPN20a localization by immunofluorescence microscopy. As such, the subcellular localization of ectopic hPTPN20a–HA was assessed in ECV304 (results not shown) and COS1 cells (Figure 5A). hPTPN20a–HA either was nuclear-targeted with a reticular cytoplasmic localization, often with concentrated staining to one side of the nucleus reminiscent of endoplasmic reticulum and Golgi apparatus respectively (approx. 60–90% of cells), or demonstrated nuclear exclusion with diffuse cytoplasmic and cell peripheral staining (Figure 5A). These expression patterns were detected even when very low amounts of hPTPN20a–HA were expressed (results not shown). The subcellular targeting of hPTPN20a–HA to membranes, cytosol and the nucleus was confirmed by immunoblot analysis of hPTPN20a–HA-expressing COS1 cells fractionated after hypotonic lysis into plasma membrane/endoplasmic reticulum, cytosol and nuclei/mitochondria/endoplasmic reticulum fractions by differential centrifugation as described in the Material and methods section. The localization of hPTPN20a–HA was compared with the localizations of the endoplasmic-reticulum-targeted PDI (protein disulphide-isomerase) and the plasma-membrane-targeted EGFR (EGF receptor) (Figure 5B). hPTPN20a–HA was present in all compartments, but was most abundant in the nuclei/mitochondria/endoplasmic reticulum fraction (Figure 5B), consistent with the predominant nuclear localization of hPTPN20a–HA in asynchronous cells (Figure 5A). Moreover, although recognition of non-specific proteins by the TT3 antibody (Figure 4) prohibited its use in assessing localization by immunofluorescence microscopy, we determined the subcellular localization of endogenous hPTPN20 by assessing its distribution in fractionated COS1 cells (Figure 5C). hPTPN20 localization was compared with the

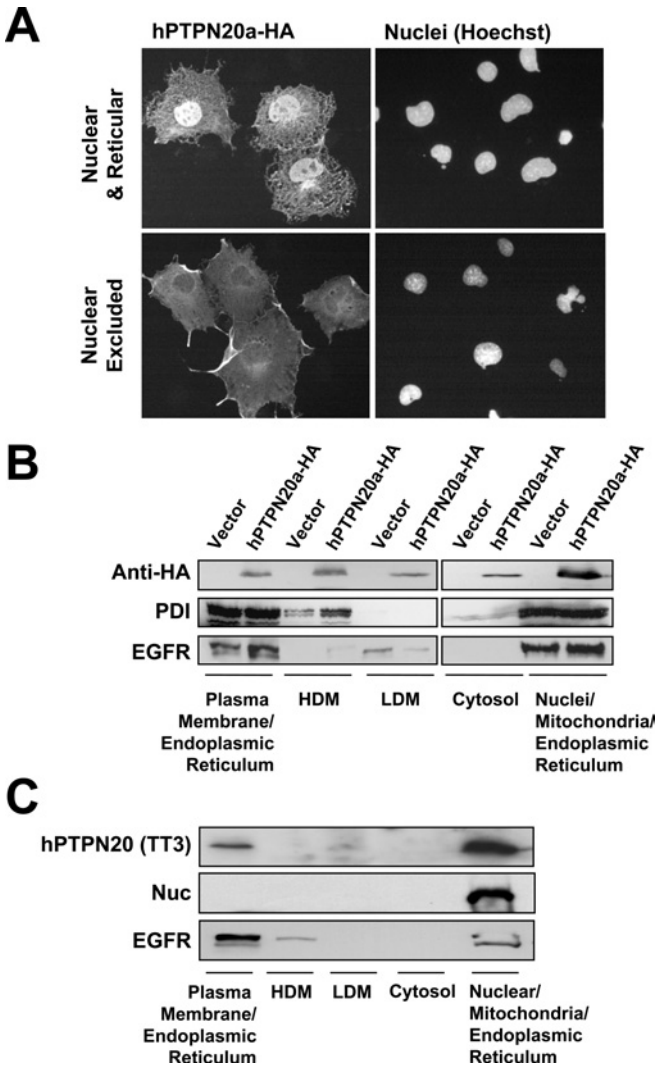

Figure 5 Divergent hPTPN20a subcellular distributions

(**A**) Asynchronous COS1 cells transiently expressing hPTPN20a–HA were processed for immunofluorescence microscopy with antibodies against HA (12CA5). Nuclei were visualized with Hoechst DNA stain. Shown are the divergent subcellular distributions of hPTPN20a–HA. (**B**) COS1 cells were transfected with vector control, or a construct for the expression hPTPN20a–HA. At 36 h post-transfection, cells were fractionated into high-density microsome (HDM), low-density microsome (LDM), cytosol, plasma membrane/endoplasmic reticulum and nuclear/mitochondrial/endoplasmic reticulum fractions as described in the Materials and methods section. Equal amounts of protein were resolved by SDS/PAGE (12% polyacrylamide) and analysed by immunoblot analysis using antibodies specific for HA (12CA5), the endoplasmic reticulum marker PDI and the EGFR, which is localized at the plasma membrane. (**C**) Asynchronous COS1 cells were fractionated as described above, and equal amounts of protein were resolved by SDS/PAGE (12% polyacrylamide) and immunoblotted with hPTPN20-specific antibodies (TT3) and antibodies specific for EGFR and the nuclear protein nucleoporin p62 (Nuc).

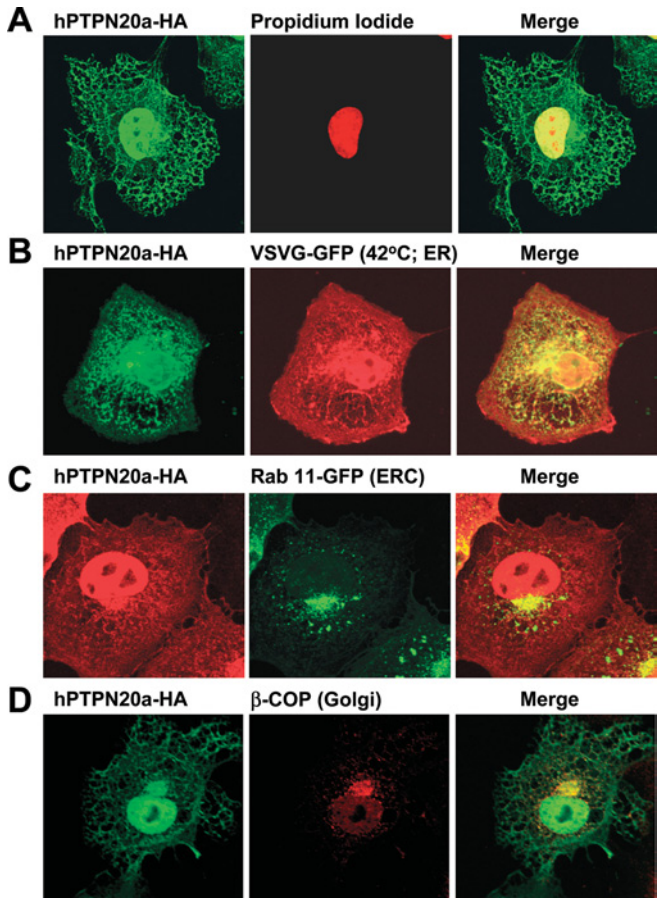

Figure 6 Localization of hPTPN20a to the nucleus, endoplasmic reticulum, Golgi apparatus and the ERC

COS1 cells transfected with (**A**) hPTPN20a-HA-pMT2 alone or with constructs expressing (**B**) VSVG–GFP [at 42 °C targeted to the endoplasmic reticulum (ER)] or (**C**) GFP–Rab11 (a marker for the ERC) were serum-starved and processed for confocal microscopy with antibodies against HA (12CA5) and (**D**) β-COP (a marker for Golgi apparatus) as indicated. In (**A**), the nucleus was visualized with propidium iodide as described in the Materials and methods section.

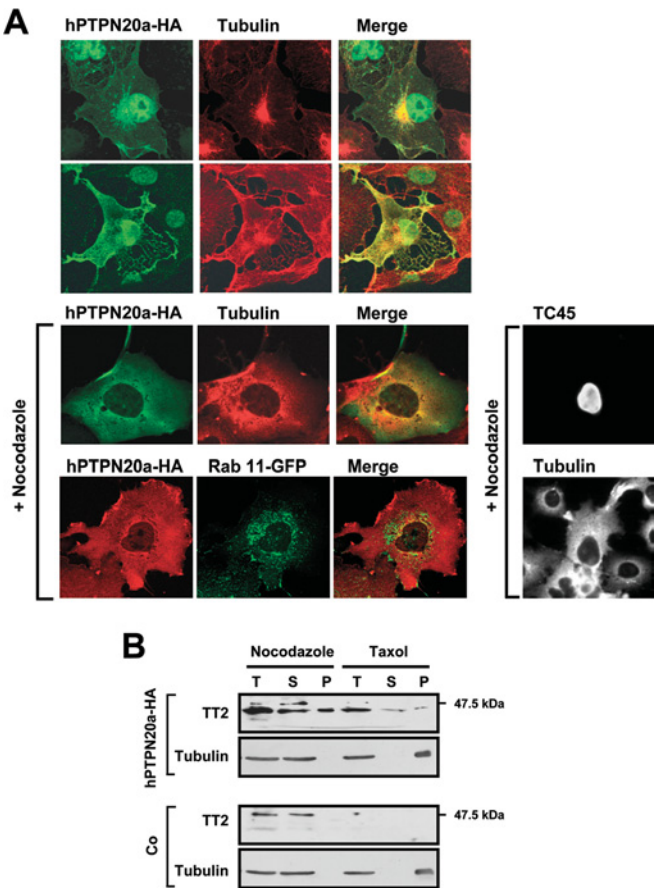

Figure 7 hPTPN20a localization is dependent on the microtubule network

(**A**) COS1 cells transfected with TC45-pMT2, hPTPN20a-HA-pMT2 alone, or hPTPN20a-HA-pMT2 and pEGFP-Rab11, were serum-starved and then either left untreated or treated with 500 ng/ml nocodazole for 5 h. Cells were then processed for confocal microscopy with polyclonal antibodies against hPTPN20a (TT2) or TC45 (159) and monoclonal anti-tubulin as indicated. (**B**) HeLa cells electroporated with pCG vector control (Co) or hPTPN20a-HA-pCG were left untreated, or were treated with the microtubule-stabilizing agent taxol or the microtubule-depolymerizing agent nocodazole as described in the Materials and methods section. Total protein (T) was extracted in microtubule-stabilizing buffer and fractionated into soluble (cytosolic fraction) (S) and insoluble proteins (microtubule fraction) (P). Proteins were resolved by SDS/PAGE (10 % polyacrylamide) and immunoblotted with antibodies against HA (12CA5) or tubulin.

distribution of the EGFR and the nuclear-restricted protein nucleoporin p62. In asynchronous cells, endogenous hPTPN20 was present in the plasma membrane/endoplasmic reticulum and the nuclear/mitochondrial/endoplasmic reticulum fractions (Figure 5C), consistent with the predominant nuclear and membrane targeting of ectopic hPTPN20a–HA (Figures 5A and 5B). Appreciable amounts of endogenous hPTPN20 were not detected in other fractions, including the cytoplasm, as was the case for ectopic hPTPN20a–HA (Figures 5B and 5C). One possibility is that the targeting of hPTPN20a to such compartments may be transient and beyond the detection capabilities of our antibodies and that the presence of exogenous hPTPN20a–HA in such fractions may be exacerbated by overexpression.

Nuclear hPTPN20–HA localization was confirmed further by confocal microscopy co-staining DNA with propidium iodide (Figure 6A). The reticular hPTPN20a–HA staining showed co-localization with markers of the endoplasmic reticulum, including calnexin and PDI (results not shown) and a GFP-fused temperature-sensitive variant of VSVG (Figure 6B) that is retained in the endoplasmic reticulum at 42 °C owing to protein misfolding [32]. In cells that had nuclear and reticular staining, the punctum of hPTPN20a staining to one of the nuclei co-localized with clathrin-coated vesicles, endosomes and the ERC (endocytic recycling compartment) [33], as indicated by its co-localization with clathrin (results not shown), co-transfected GFP–Rab5 (results not shown) and co-transfected GFP–Rab11 respectively (Figure 6C). In addition, the punctum of hPTPN20a staining also co-localized with the Golgi apparatus, as indicated by its co-localization with β-COP (Figure 6D) and a co-transfected GFP-fusion protein of the GTPase Rab6 (results not shown).

The structural integrity and the trafficking of molecules between subcellular compartments including Golgi, endoplasmic reticulum and endosomes is dependent on the organelles being tethered to microtubules which emanate from the MTOC (microtubule-organizing centre) [34–36]. The punctum of hPTPN20a–HA staining that was to one side of the nucleus and the reticular hPTPN20a–HA staining co-localized with the microtubule network and the MTOC respectively (Figure 7A, top panel). Dispersal of the MTOC and microtubules with the depolymerizing agent nocodazole disseminated the clathrin-coated vesicles (results not shown) and the ERC as indicated by the redistribution of GFP–Rab11 from the perinuclear localization evident in Figure 6(C) (Figure 7A, bottom panel). In cells treated with nocodazole, hPTPN20a had a diffuse cytoplasmic staining and did

not co-localize with clathrin (results not shown) or GFP–Rab11 vesicular structures [33,37] (Figure 7A, bottom panel), indicating that hPTPN20a did not interact directly with endosomal compartments. In addition, in nocodazole-treated cells, hPTPN20a was excluded from the nucleus in more than 90 % of cells (Figure 7A, bottom panel). In contrast, TC45 remained in the nucleus (Figure 7A), demonstrating that nuclear structural integrity was maintained in the presence of nocozadole. These results indicate that hPTPN20a localization may be dependent on the microtubule network. However, hPTPN20a–HA does not associate directly with microtubules, since hPTPN20a–HA did not co-fractionate with depolymerized tubulin from nocodazole-treated cells or with bundled microtubules from taxol-treated cells (Figure 7B). Taken together, these results indicate that hPTPN20a might be targeted to microtubules and that its association might be dynamic, allowing for trafficking to various subcellular compartments.

hPTPN20a is targeted to sites of actin polymerization

Given the presence of two distinct hPTPN20a–HA subcellular distributions in asynchronous cells, we reasoned that specific cellular stimuli might alter hPTPN20a localization. We noted that the microtubule- and nuclear-targeted localization of hPTPN20a predominated in serum-starved COS1 cells (results not shown). However, in response to 1-100 ng/ml EGF stimulation, hPTPN20a underwent a dramatic change in localization and was excluded from the nucleus, showing diffuse cytoplasmic staining and prominent cell peripheral staining (Figure 8A). The cell peripheral staining co-localized with cortical actin (results not shown) and actin in membrane ruffles, sites highly enriched in dynamic actin polymerization (Figure 8B). A similar dynamic change in localization was noted in response to hyperosmotic shock (600 mM sorbitol) (Figure 8A) and here we noted distinct puncta of hPTPN20a–HA staining at the cell periphery that co-localized with actin (Figure 8B). In addition, treatment of cells with pervanadate, which inhibits PTPs and promotes tyrosine-phosphorylation-dependent signalling, also resulted in a dramatic change in localization with prominent cell peripheral staining (Figure 8A). Finally, hPTPN20a–HA also localized to membrane ruffles (results not shown) and sites enriched in actin in cells that were detached and subsequently allowed to spread on the extracellular matrix protein fibronectin (Figure 8B). Taken together, these results indicate that hPTPN20a is targeted to sites of dynamic actin polymerization in response to varied extracellular stimuli.

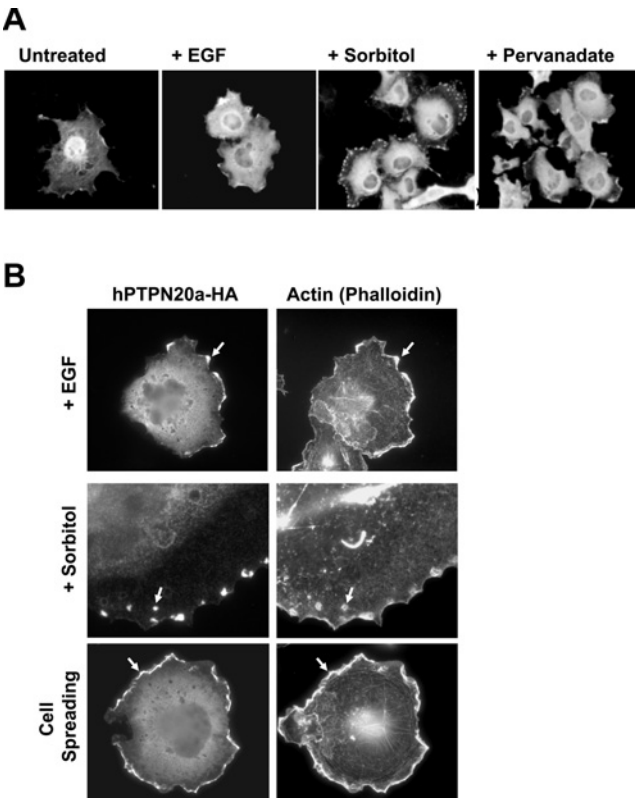

Figure 8 hPTPN20a is excluded from the nucleus and targeted to sites of actin polymerization in response to various stimuli

COS1 cells transfected with hPTPN20a-HA-pMT2 were serum-starved and were left untreated, or were stimulated with 10 ng/ml EGF for 15 min, 600 mM sorbitol for 60 min or 200 μM pervanadate for 15 min, and then processed for immunofluorescence microscopy with antibodies against HA (12CA5). (**B**) COS1 cells transfected with hPTPN20a-HA-pMT2 were serum-starved and stimulated with EGF or sorbitol as indicated above, or otherwise detached and allowed to spread on fibronectin-coated coverslips as described in the Materials and methods section. Cells were processed for immunofluorescence microscopy with antibodies against HA and Texas-Red Phalloidin to detect actin. Representative sites enriched in actin demonstrating co-localization with hPTPN20a–HA are indicated by arrows.

DISCUSSION

In recent years, biochemical, structural and genetic studies have illustrated that PTPs can be highly specific enzymes *in vivo*, integral to the regulation of fundamental cellular responses [1,38]. Despite their pivotal roles in such cellular processes, most PTP family members remain poorly characterized. In the present study, we have undertaken a characterization of the classical human PTP family member hPTPN20. We report that alternative splicing of the *PTPN20* gene can result in the expression of at least 22 mRNA transcripts, including 18 novel sequences that encode 16 potential variant proteins making *PTPN20* one the most alternatively spliced PTP genes currently known.

Northern blot analysis of human tissues suggested that *PTPN20* mRNA is not abundant and that its expression is highest in human testes, consistent with a previous report characterizing the expression of the putative hPTPN20b murine homologue Typ [29]. However, the existence of *PTPN20* ESTs from various human tissues, together with our RT-PCR and immunoblot analyses, suggests that the phosphatase may be widely expressed, albeit at lower levels than those found in testes. Our RT-PCR analyses indicated that the *PTPN20a* mRNA may predominate in cultured cells, and, consistent with this, hPTPN20-specific antibodies detected a protein with the predicted molecular mass of hPTPN20a in all cell lines examined.

To provide insight into the possible functions of hPTPN20a, we assessed its subcellular distribution by immunofluorescence microscopy. We found that the subcellular localization of hPTPN20a was dependent on an intact microtubule network. hPTPN20a localized to the microtubules and the MTOC, and co-localized with organelles such as the Golgi apparatus and the endoplasmic reticulum whose organization/structure is dependent on microtubule integrity [34–36]. Moreover, although hPTPN20a lacks any discernable nuclear localization sequence, it was targeted to the nucleus. Importantly, microtubule disruption not only resulted in hPTPN20a adopting a diffuse cytoplasmic localization, but also in exclusion of hPTPN20a from the nucleus. Previous studies have demonstrated that various proteins including the tumour-suppressor protein p53 [39] and the parathyroid-hormone-related protein [40] utilize microtubules to traffic to the nucleus and we propose that same may be true for hPTPN20a.

hPTPN20a underwent a dramatic change in localization in response to varied extracellular stimuli including hyperosmotic

shock, EGF and cell spreading. Under these conditions, hPTPN20a was targeted to sites of dynamic actin polymerization, including membrane ruffles and cortical actin and was excluded from the nucleus without discernable microtubule targeting. These results are consistent with hPTPN20a having a dynamic subcellular localization, and we propose that hPTPN20a might recognize a distinct substrate at sites of actin polymerization. Notably, our preliminary studies indicate that hPTPN20a is very specific in its substrate recognition, since its overexpression had no discernable effect on EGFR phosphorylation or signalling (results not shown). Moreover, we have not detected any tyrosyl phosphorylated proteins associated with hPTPN20a-D314A 'substrate-trapping' mutants [18,41] in response to either EGF or sorbitol in COS1 cells (results not shown), indicating that hPTPN20a substrates may not be abundant and/or that their stoichiometry of phosphorylation may be low. Nonetheless, the pronounced accumulation of hPTPN20a to sites of polymerized actin is consistent with the phosphatase having a role in the modulation of actin dynamics or in cellular processes dependent on cytoskeletal reorganization, but further studies are needed to address this.

Our studies indicate that alternative splicing of the *PTPN20* gene can generate mRNA transcripts that encode proteins lacking functional PTP catalytic domains. Two other PTP genes, encoding the intracellular STEP (striatal enriched phosphatase) [42,43] and the transmembrane receptor-like RPTPζ/β [44–46] are alternatively spliced to generate proteins that lack catalytic domains. No information is available as to the function of the STEP variant [42,43], but the RPTPζ/β variant is secreted and may have distinct, as well as competitive, possibly dominant-negative, functions with respect to full-length transmembrane RPTPζ/β [47–51]. The predicted PTP domain 'null' hPTPN20 variants may also act as dominant negatives, as suggested not only for the RPTPζ/β variant, but also for the naturally occurring PTP inactive or phosphatase 'dead' so-called STYX-like (phosphoserine/threonine/tyrosine-interacting) proteins [47–52]. Notably, the archetypal phosphatase 'dead' STYX protein is essential *in vivo*, and mice lacking STYX are defective in sperm production and are infertile [53]. Even though we did not detect significant levels of the PTP domain 'null' hPTPN20 variants in the cell lines tested, it is possible that such proteins may nevertheless exist *in vivo* and further studies are needed to assess their expression under conditions not emulated by asynchronous cells *in vitro*. Although the biological roles of hPTPN20 remain to be elucidated, our results underscore the complexity of PTP regulation and function and provide a basis from which to begin a systematic examination.

We thank E. Baker for FISH analysis, P. E. Bukczynska for technical assistance, and M. T. Gillespie for helpful discussions. This work was supported by the Australian Research Council. T. T. is a Monash University Logan Fellow.

REFERENCES

1 Tonks, N. K. and Neel, B. G. (2001) Combinatorial control of the specificity of protein tyrosine phosphatases. Curr. Opin. Cell Biol. **13**, 182–195

2 Andersen, J. N., Mortensen, O. H., Peters, G. H., Drake, P. G., Iversen, L. F., Olsen, O. H., Jansen, P. G., Andersen, H. S., Tonks, N. K. and Moller, N. P. (2001) Structural and evolutionary relationships among protein tyrosine phosphatase domains. Mol. Cell. Biol. **21**, 7117–7136

3 Andersen, J. N., Jansen, P. G., Echwald, S. M., Mortensen, O. H., Fukada, T., Del Vecchio, R., Tonks, N. K. and Moller, N. P. (2004) A genomic perspective on protein tyrosine phosphatases: gene structure, pseudogenes, and genetic disease linkage. FASEB J. **18**, 8–30

4 Ponniah, S., Wang, D. Z., Lim, K. L. and Pallen, C. J. (1999) Targeted disruption of the tyrosine phosphatase PTPα leads to constitutive downregulation of the kinases Src and Fyn. Curr. Biol. **9**, 535–538

5 Zheng, X. M., Resnick, R. J. and Shalloway, D. (2000) A phosphotyrosine displacement mechanism for activation of Src by PTPα. EMBO J. **19**, 964–978

6 Zhang, S. Q., Yang, W., Kontaridis, M. I., Bivona, T. G., Wen, G., Araki, T., Luo, J., Thompson, J. A., Schraven, B. L., Philips, M. R. and Neel, B. G. (2004) Shp2 regulates SRC family kinase activity and Ras/Erk activation by controlling Csk recruitment. Mol. Cell **13**, 341–355

7 Ruivenkamp, C. A., van Wezel, T., Zanon, C., Stassen, A. P., Vlcek, C., Csikos, T., Klous, A. M., Tripodis, N., Perrakis, A., Boerrigter, L. et al. (2002) PTPRJ is a candidate for the mouse colon-cancer susceptibility locus Scc1 and is frequently deleted in human cancers. Nat. Genet. **31**, 295–300

8 Wang, Z., Shen, D., Parsons, D. W., Bardelli, A., Sager, J., Szabo, S., Ptak, J., Silliman, N., Peters, B. A., van der Heijden, M. S. et al. (2004) Mutational analysis of the tyrosine phosphatome in colorectal cancers. Science **304**, 1164–1166

9 Bentires-Alj, M., Paez, J. G., David, F. S., Keilhack, H., Halmos, B., Naoki, K., Maris, J. M., Richardson, A., Bardelli, A., Sugarbaker, D. J. et al. (2004) Activating mutations of the noonan syndrome-associated SHP2/PTPN11 gene in human solid tumors and adult acute myelogenous leukemia. Cancer Res. **64**, 8816–8820

10 Mohi, M. G., Williams, I. R., Dearolf, C. R., Chan, G., Kutok, J. L., Cohen, S., Morgan, K., Boulton, C., Shigematsu, H., Keilhack, H. et al. (2005) Prognostic, therapeutic, and mechanistic implications of a mouse model of leukemia evoked by Shp2 (PTPN11) mutations. Cancer Cell **7**, 179–191

11 Ahmad, F., Considine, R. V. and Goldstein, B. J. (1995) Increased abundance of the receptor-type protein-tyrosine phosphatase LAR accounts for the elevated insulin receptor dephosphorylating activity in adipose tissue of obese human subjects. J. Clin. Invest. **95**, 2806–2812

12 Ahmad, F., Azevedo, J. L., Cortright, R., Dohm, G. L. and Goldstein, B. J. (1997) Alterations in skeletal muscle protein-tyrosine phosphatase activity and expression in insulin-resistant human obesity and diabetes. J. Clin. Invest. **100**, 449–458

13 Bottini, N., Musumeci, L., Alonso, A., Rahmouni, S., Nika, K., Rostamkhani, M., MacMurray, J., Meloni, G. F., Lucarelli, P., Pellecchia, M. et al. (2004) A functional variant of lymphoid tyrosine phosphatase is associated with type I diabetes. Nat. Genet. **36**, 337–338

14 Kung, C., Pingel, J. T., Heikinheimo, M., Klemola, T., Varkila, K., Yoo, L. I., Vuopala, K., Poyhonen, M., Uhari, M., Rogers, M. et al. (2000) Mutations in the tyrosine phosphatase CD45 gene in a child with severe combined immunodeficiency disease. Nat. Med. **6**, 343–345

15 Araki, T., Mohi, M. G., Ismat, F. A., Bronson, R. T., Williams, I. R., Kutok, J. L., Yang, W., Pao, L. I., Gilliland, D. G., Epstein, J. A. and Neel, B. G. (2004) Mouse model of Noonan syndrome reveals cell type- and gene dosage-dependent effects of Ptpn11 mutation. Nat. Med. **10**, 849–857

16 Higashi, H., Tsutsumi, R., Muto, S., Sugiyama, T., Azuma, T., Asaka, M. and Hatakeyama, M. (2002) SHP-2 tyrosine phosphatase as an intracellular target of *Helicobacter pylori* CagA protein. Science **295**, 683–686

17 Fujikawa, A., Shirasaka, D., Yamamoto, S., Ota, H., Yahiro, K., Fukada, M., Shintani, T., Wada, A., Aoyama, N., Hirayama, T. et al. (2003) Mice deficient in protein tyrosine phosphatase receptor type Z are resistant to gastric ulcer induction by VacA of *Helicobacter pylori*. Nat. Genet. **33**, 375–381

18 Tiganis, T., Bennett, A. M., Ravichandran, K. S. and Tonks, N. K. (1998) Epidermal growth factor receptor and the adaptor protein p52^{Shc} are specific substrates of T-cell protein tyrosine phosphatase. Mol. Cell. Biol. **18**, 1622–1634

19 Brummelkamp, T. R., Bernards, R. and Agami, R. (2002) A system for stable expression of short interfering RNAs in mammalian cells. Science **296**, 550–553

20 Bukczynska, P., Klingler-Hoffmann, M., Mitchelhill, K. I., Lam, M. H., Ciccomancini, M., Tonks, N. K., Sarcevic, B., Kemp, B. E. and Tiganis, T. (2004) The T-cell protein tyrosine phosphatase is phosphorylated on Ser-304 by cyclin-dependent protein kinases in mitosis. Biochem. J. **380**, 939–949

21 Brown, J., Reading, S. J., Jones, S., Fitchett, C. J., Howl, J., Martin, A., Longland, C. L., Michelangeli, F., Dubrova, Y. E. and Brown, C. A. (2000) Critical evaluation of ECV304 as a human endothelial cell model defined by genetic analysis and functional responses: a comparison with the human bladder cancer derived epithelial cell line T24/83. Lab. Invest. **80**, 37–45

22 Suda, K., Rothen-Rutishauser, B., Gunthert, M. and Wunderli-Allenspach, H. (2001) Phenotypic characterization of human umbilical vein endothelial (ECV304) and urinary carcinoma (T24) cells: endothelial versus epithelial features. In Vitro Cell. Dev. Biol. Anim. **37**, 505–514

23 Tiganis, T., Kemp, B. E. and Tonks, N. K. (1999) The protein tyrosine phosphatase TCPTP regulates epidermal growth factor receptor-mediated and phosphatidylinositol 3-kinase-dependent signalling. J. Biol. Chem. **274**, 27768–27775

24 Klingler-Hoffmann, M., Fodero-Tavoletti, M. T., Mishima, K., Narita, Y., Cavenee, W. K., Furnari, F. B., Huang, H. J. and Tiganis, T. (2001) The protein tyrosine phosphatase TCPTP suppresses the tumorigenicity of glioblastoma cells expressing a mutant epidermal growth factor receptor. J. Biol. Chem. **276**, 46313–46318

25 Simpson, I. A., Yver, D. R., Hissin, P. J., Wardzala, L. J., Karnieli, E., Salans, L. B. and Cushman, S. W. (1983) Insulin-stimulated translocation of glucose transporters in the isolated rat adipose cells: characterization of subcellular fractions. Biochim. Biophys. Acta **763**, 393–407
26 Hao, L., Tiganis, T., Tonks, N. K. and Charbonneau, H. (1997) The non-catalytic C-terminal segment of the T cell protein tyrosine phosphatase regulates activity via an intramolecular mechanism. J. Biol. Chem. **272**, 29322–29329
27 Villalba, M., Wente, S. R., Russell, D. S., Ahn, J. C., Reichelderfer, C. F. and Rosen, O. M. (1989) Another version of the human insulin receptor kinase domain: expression, purification, and characterization. Proc. Natl. Acad. Sci. U.S.A. **86**, 7848–7852
28 Takahashi, T., Takahashi, K., St John, P. L., Fleming, P. A., Tomemori, T., Watanabe, T., Abrahamson, D. R., Drake, C. J., Shirasawa, T. and Daniel, T. O. (2003) A mutant receptor tyrosine phosphatase, CD148, causes defects in vascular development. Mol. Cell. Biol. **23**, 1817–1831
29 Ohsugi, M., Kuramochi, S., Matsuda, S. and Yamamoto, T. (1997) Molecular cloning and characterization of a novel cytoplasmic protein-tyrosine phosphatase that is specifically expressed in spermatocytes. J. Biol. Chem. **272**, 33092–33099
30 Shapiro, M. B. and Senapathy, P. (1987) RNA splice junctions of different classes of eukaryotes: sequence statistics and functional implications in gene expression. Nucleic Acids Res. **15**, 7155–7174
31 Rechsteiner, M. and Rogers, S. W. (1996) PEST sequences and regulation by proteolysis. Trends Biochem. Sci. **21**, 267–271
32 Nehls, S., Snapp, E. L., Cole, N. B., Zaal, K. J., Kenworthy, A. K., Roberts, T. H., Ellenberg, J., Presley, J. F., Siggia, E. and Lippincott-Schwartz, J. (2000) Dynamics and retention of misfolded proteins in native ER membranes. Nat. Cell Biol. **2**, 288–295
33 Maxfield, F. R. and McGraw, T. E. (2004) Endocytic recycling. Nat. Rev. Mol. Cell Biol. **5**, 121–132
34 Matteoni, R. and Kreis, T. E. (1987) Translocation and clustering of endosomes and lysosomes depends on microtubules. J. Cell. Biol. **105**, 1253–1265
35 Du, Y., Ferro-Novick, S. and Novick, P. (2004) Dynamics and inheritance of the endoplasmic reticulum. J. Cell. Sci. **117**, 2871–2878
36 Allan, V. J., Thompson, H. M. and McNiven, M. A. (2002) Motoring around the Golgi. Nat. Cell Biol. **4**, E236–E242
37 Ren, M., Xu, G., Zeng, J., De Lemos-Chiarandini, C., Adesnik, M. and Sabatini, D. D. (1998) Hydrolysis of GTP on rab11 is required for the direct delivery of transferrin from the pericentriolar recycling compartment to the cell surface but not from sorting endosomes. Proc. Natl. Acad. Sci. U.S.A. **95**, 6187–6192
38 Tonks, N. K. (2003) PTP1B: from the sidelines to the front lines! FEBS Lett. **546**, 140–148
39 Giannakakou, P., Sackett, D. L., Ward, Y., Webster, K. R., Blagosklonny, M. V. and Fojo, T. (2000) p53 is associated with cellular microtubules and is transported to the nucleus by dynein. Nat. Cell Biol. **2**, 709–717
40 Lam, M. H., Thomas, R. J., Loveland, K. L., Schilders, S., Gu, M., Martin, T. J., Gillespie, M. T. and Jans, D. A. (2002) Nuclear transport of parathyroid hormone (PTH)-related protein is dependent on microtubules. Mol. Endocrinol. **16**, 390–401
41 Flint, A. J., Tiganis, T., Barford, D. and Tonks, N. K. (1997) Development of "substrate-trapping" mutants to identify physiological substrates of protein tyrosine phosphatases. Proc. Natl. Acad. Sci. U.S.A. **94**, 1680–1685
42 Sharma, E., Zhao, F. S., Bult, A. and Lombroso, P. J. (1995) Identification of two alternatively spliced transcripts of STEP: a subfamily of brain-enriched protein tyrosine phosphatases. Mol. Brain Res. **32**, 87–93
43 Bult, A., Zhao, F., Dirkx, Jr, R., Raghunathan, A., Solimena, M. and Lombroso, P. J. (1997) STEP: a family of brain-enriched PTPs. Alternative splicing produces transmembrane, cytosolic and truncated isoforms. Eur. J. Cell Biol. **72**, 337–344
44 Maurel, P., Meyer-Puttlitz, B., Flad, M., Margolis, R. U. and Margolis, R. K. (1995) Nucleotide sequence and molecular variants of rat receptor-type protein tyrosine phosphatase-ζ/β. DNA Seq. **5**, 323–328
45 Barnea, G., Grumet, M., Milev, P., Silvennoinen, O., Levy, J. B., Sap, J. and Schlessinger, J. (1994) Receptor tyrosine phosphatase β is expressed in the form of proteoglycan and binds to the extracellular matrix protein tenascin. J. Biol. Chem. **269**, 14349–14352
46 Krueger, N. X. and Saito, H. (1992) A human transmembrane protein-tyrosine-phosphatase, PTPζ, is expressed in brain and has an N-terminal receptor domain homologous to carbonic anhydrases. Proc. Natl. Acad. Sci. U.S.A. **89**, 7417–7421
47 Maeda, N. and Noda, M. (1996) 6B4 proteoglycan/phosphacan is a repulsive substratum but promotes morphological differentiation of cortical neurons. Development **122**, 647–658
48 Sakurai, T., Friedlander, D. R. and Grumet, M. (1996) Expression of polypeptide variants of receptor-type protein tyrosine phosphatase β: the secreted form, phosphacan, increases dramatically during embryonic development and modulates glial cell behavior *in vitro*. J. Neurosci. Res. **43**, 694–706
49 Nishiwaki, T., Maeda, N. and Noda, M. (1998) Characterization and developmental regulation of proteoglycan-type protein tyrosine phosphatase ζ/RPTPβ isoforms. J. Biochem. (Tokyo) **123**, 458–467
50 Maeda, N. and Noda, M. (1998) Involvement of receptor-like protein tyrosine phosphatase ζ/RPTPβ and its ligand pleiotrophin/heparin-binding growth-associated molecule (HB-GAM) in neuronal migration. J. Cell. Biol. **142**, 203–216
51 Canoll, P. D., Petanceska, S., Schlessinger, J. and Musacchio, J. M. (1996) Three forms of RPTP-β are differentially expressed during gliogenesis in the developing rat brain and during glial cell differentiation in culture. J. Neurosci. Res. **44**, 199–215
52 Wishart, M. J. and Dixon, J. E. (1998) Gathering STYX: phosphatase-like form predicts functions for unique protein-interaction domains. Trends Biochem. Sci. **23**, 301–306
53 Wishart, M. J. and Dixon, J. E. (2002) The archetype STYX/dead-phosphatase complexes with a spermatid mRNA-binding protein and is essential for normal sperm production. Proc. Natl. Acad. Sci. U.S.A. **99**, 2112–2117

Received 19 November 2004/23 March 2005; accepted 24 March 2005
Published as BJ Immediate Publication 24 March 2005, DOI 10.1042/BJ20041932